Hindawi
Geofluids
Volume 2023, Article ID 3115884, 13 pages
https://doi.org/10.1155/2023/3115884

Research Article

Characteristics of Tight Dolostone Reservoir and Its Main Controlling Factors in the Submember $Ma5_5$ of Majiagou Formation in the Western Ordos Basin

Baiqiang Li,[1,2] **Taofa Zhou**,[1,2] **Zhenzhen Wu**,[3] **Yanick Blaise Ketchaya**,[1,2] **Qicong Wang**,[3] **Xiaoli Zhang**,[4] **Jiangmin Du**,[5] **and Jonathan Atuquaye Quaye**[6]

[1]*Ore Deposit and Exploration Centre (ODEC), School of Resources and Environmental Engineering, Hefei University of Technology, Hefei 230009, China*
[2]*Anhui Province Engineering Research Center for Mineral Resources and Mine Environments, Hefei, 230009 Anhui, China*
[3]*School of Earth Sciences and Engineering/Shaanxi Key Laboratory of Petroleum Accumulation Geology, Xi'an Shiyou University, Xi'an 710065, China*
[4]*Department of Geology, Northwest University, Xi'an 710069, China*
[5]*Hebei Key Laboratory of Strategic Critical Mineral Resources, Hebei GEO University, Shijiazhuang 050031, China*
[6]*Department of Petroleum Engineering, Faculty of Civil and Geo-Engineering, College of Engineering, Kwame Nkrumah University of Science and Technology, Kumasi, Ghana*

Correspondence should be addressed to Baiqiang Li; 924374439@qq.com

Received 10 November 2022; Revised 8 December 2022; Accepted 31 March 2023; Published 20 April 2023

Academic Editor: Yang Wang

The tight carbonate reservoir was controlled by various geological factors, and such factors played different roles in buried depths and formations. Therefore, studies related to the factors controlling carbonate reservoir distribution are of great significance for the prediction and evaluation of high-quality dolostone reservoirs. In this paper, we focus on the controlling factor of the submember $Ma5_5$ dolostone reservoir in the western Ordos Basin. The main rock types, reservoir pores, physical properties, and pore structure characteristics of the reservoir were analyzed by thin section identification, physical property analysis, and mercury injection, respectively. Then, the main controlling factors of reservoir development were comprehensively analyzed from the perspectives of palaeostructure, lithofacies palaeogeography, diagenesis, and diagenetic facies. The results show that two kinds of dolostone reservoirs in the submember $Ma5_5$ developed in the western Ordos Basin, including intercrystalline pore-type and dissolution pore-type. The former reservoir is primarily characterized by powder-fine dolostone with residual structure, dolomite intercrystalline pore, and micropore with porosity ranging from 2% to 11%. There are three types of pore structures developed in it, such as macropore-medium throat-single peak (MAMS), macropore-fine throat-single peak (MAFS), and medium pore-fine throat-single peak (MEFS). The latter reservoir is mainly featured by powdery crystalline dolostone with gypsum and halite dissolution, moldic pore, and dissolved pore between breccias with a porosity greater than 5%. It consists of two types of pore structures, such as macropore-fine throat-single peak (MAFS) and medium pore-coarse throat-multipeak (MECM). The intercrystalline pore-type dolostone reservoir is mainly controlled by the lithofacies palaeogeographic environment and diagenesis. In specific, the shoal microfacies at the edge of the platform and the active reflux seepage dolomitization are the basic sedimentary environment conditions for reservoir formation and the key to reservoir formation, respectively. The dissolution pore-type dolostone reservoir is primarily influenced by both paleostructure and diagenesis. The relatively high part of the paleostructure provides favorable conditions for the formation of evaporate minerals, and early freshwater dissolution is the key to reservoir formation. This research will provide a theoretical basis for forecasting the favorable distribution areas of different types of dolostone reservoirs.

1. Introduction

The tight carbonate reservoir controlled by various geological factors [1], such as the lithofacies paleogeographic environment [2–6], karst paleomorphology [7–14], diagenesis and diagenetic facies [15–19], and tectonic movement [7, 20], is complex in rock structure with diverse reservoir pores and strong heterogeneity. However, different factors are controlling the reservoir distribution in various depths from the surface to the bottom; for example, the upper Majiagou formation may be greatly affected by karst palaeogeomorphology, while the lower Majiagou formation is highly influenced by lithofacies and the paleogeographic environment [21–23]. Thus, studies related to the factors controlling carbonate reservoir distribution are of great significance, especially for the prediction and evaluation of high-quality dolostone reservoirs [22].

After the Caledonian movement, the Lower Paleozoic Ordovician strata in Ordos Basin were uplifted and exposed to the near-surface environment and then subjected to weathering, leaching, and erosion for nearly 150 Ma or more [24]. These conditions involved the formation of karst weathering reservoirs with abundant dissolved pores at the top of the Majiagou formation [25]. The formation of several Lower Paleozoic giant gas fields such as the Daniudi [26–28], Jingbian [29, 30], Sulige, and Yulin gas fields are closely related to the development of this karst-weathered shell reservoir. In recent years, the major exploration breakthroughs of Paleozoic natural gas in the Daniudi and Jingbian gas fields accelerated the gradual expansion of Paleozoic natural gas exploration to the west of the Ordos Basin.

In recent years, many research works have been done on the factors controlling the dolostone reservoir in submember $Ma5_5$ [14, 15, 17, 18, 22, 30, 31]. These factors still remain controversial in different areas, such as the karst paleogeomorphology plays a more important role than the sedimentary environment, dolostone distribution, and diagenesis in the Daniudi gas field, but in the Sulige gas field, the sedimentary environment and diagenesis take more effects than karst paleogeomorphology [31]. So, understanding the main controlling factors for the dolostone reservoir developed in different areas is of great significance for forecasting favorable reservoir distribution.

In this paper, the aim of the research will be to focus on the controlling factors of the submember $Ma5_5$ dolostone reservoir in the western Ordos Basin. The main rock types, reservoir pore, physical properties, and pore structure characteristics of a dolostone reservoir were analyzed by drilling core observation, thin section identification, physical property analysis, and a mercury injection test, respectively. Then, the main controlling factors of reservoir development were comprehensively analyzed from the perspectives of palaeostructure, lithofacies palaeogeography, diagenesis, and diagenetic facies. This research will provide a theoretical basis for forecasting the favorable areas of different dolostone reservoir types in the Ordos Basin.

2. Geological Setting

During the sedimentary period of the Ordovician Majiagou formation, the whole structure of the Ordos Basin was composed of depression and uplift [32]. In this period and for a long time, the central palaeouplift in the southwest of the basin coexists and interacts with the northern Shaanxi depression in the east. This condition controlled the patterns of palaeostructure and paleogeographic environment of the basin [33]. In the early Paleozoic, the basin entered a stable period of craton development, and a set of marine carbonate formations was deposited with a stable distribution in the Ordos Basin [34]. Based on lithology changes, the Majiagou formation can be divided into six members, namely, Ma1 to Ma6 from bottom to top. The member Ma5 can be further divided into ten submembers from top to bottom, namely, $Ma5_1$ to $Ma5_{10}$. Among which, the $Ma5_5$ submember is a set of carbonate rocks dominated by limestone interbedded with dolostone that formed during the process of the third sea level declining while the fourth sea level rising.

The Ordos Basin positioned in central and western China (Figure 1(a)) can be divided into six tectonic units. The study area belonging to the western Yishan slope has a scope that extends from Wuqi in the west to Jingbian in the east, from the S21 well in the north to Zhidan in the south (Figure 1(b)). From top to bottom, the submember $Ma5_5$ can be divided into three lithologic sections such as limestone, dolostone, and limestone with a variable thickness of 10, 8, and 8 m, respectively. The dolostone section is a door open on natural gas exploration and is mainly formed in the declining process of the fifth relative sea level (Figure 1(c)).

3. Material and Analytical Methods

3.1. Samples. The dolostone samples were mainly collected from cores of submember $Ma5_5$ in wells S21, S22, S167, S188, and T6 in the northern area; Cc1 and Y404 in the central area; and Y580, Y402, Y1117, Y437, Y408, Y290, Y406, Y290, Y1113, Y157, and S290 in the southern area of the northwestern Ordos Basin. The sampling covers scope almost represents the whole study area. The lithology involved in the test samples mainly includes dolomicrite and powder-fine crystalline dolostone.

3.2. Whole Rock X-Ray Diffraction. The volume contents of dolomite, calcite, anhydrite, quartz, and pyrite were determined by whole-rock X-ray diffraction analysis. This analysis was completed in the State Engineering Laboratory of low-permeability oil and gas field exploration and development in Changqing Oilfield Company of China National Petroleum Corporation. The test standard used for analysis is SY/T 6210-1996, with a data accuracy of 0.01% [35].

3.3. Micropetrographic Analysis. The rock structure and pore characteristics in the dolostone samples were analyzed using core observations and thin section identification. In this work, 100 samples were analyzed for micropetrographic study. Before observing the thin sections, a staining solution mixed with aizarin red and potassium ferricyanide was

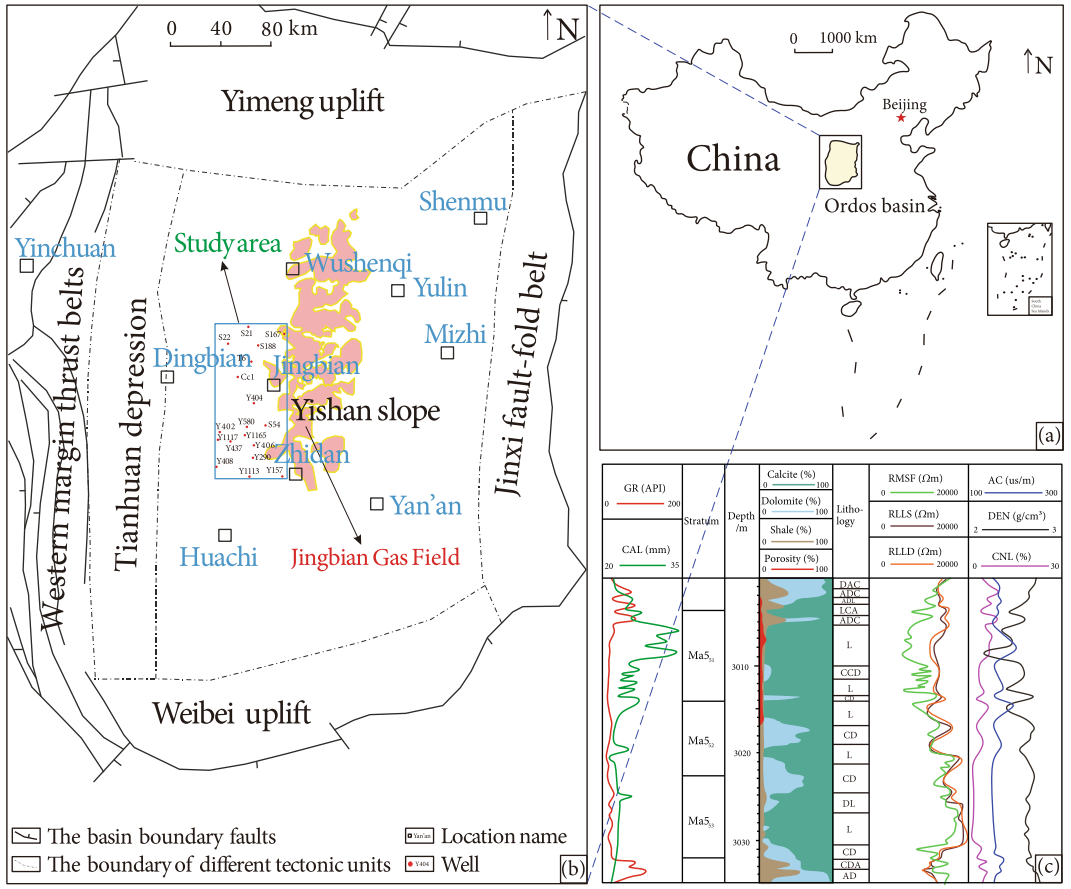

FIGURE 1: Geological settings of the western Ordos Basin. ((a) Location of the Ordos Basin. (b) Structural units, location of the study area, and sampling wells. (c). The comprehensive stratigraphic column of submember $Ma5_5$).

injected into rock pores. Then, a high-power microscope (DMLP-217400) was used to identify rock structure and pore characteristics. These analyses were conducted at the School of Resources and Environmental Engineering, Hefei University of Technology. The detection standard used was SY/T5368-2000, and all of the samples were analyzed at room temperature.

4. Results

4.1. Main Reservoir Types and Their Characteristics. Based on the genetic-structural classification scheme of carbonate rock [36], the dolostone reservoir rock types of the submember $Ma5_5$ in the study area were divided into two types in combination with the mineral composition, diagenesis, and sedimentary texture and structure. As a result, the reservoir type mainly includes intercrystalline pore-type dolostone reservoir and dissolution pore-type dolostone reservoir.

4.1.1. Intercrystalline Pore-Type Dolostone Reservoir

(1) Petrological Characteristics of Reservoir. The major rock type in this kind of reservoir is powder-fine crystalline dolostone with residual texture. It can be subdivided in combination with the composition, sedimentary, and diagenetic structures of the rock, into powder-fine oolitic dolostone with residual sand-cutting texture, powder-fine calcite-containing dolostone with chondrum structure, and powder-crystal dolostone with residual gravel texture. The dolomite content of powder-fine crystalline dolostone with residual texture is generally greater than 90%. Most dolomite is powder and fine crystals with a grain size between 0.005 and 0.25 mm. They have a relatively high automorphism degree with a dolomite order degree in the range of 0.7 to 0.85. In addition, particular residual texture and some reducing minerals also can be observed in the rocks, such as oolitic texture, isolated pyrites (Figure 2(a)), chondrum texture (Figure 2(b)), and sand and gravel debris.

(2) Pore Types and Their Genesis. The two major pore types involved in powder-fine crystalline dolostone with residual texture are intercrystalline pore and micropore. They are developed in powder-fine dolostone with residual sand-cutting texture and powder-crystal dolostone with residual gravel texture, respectively.

Intercrystalline pores are generally densely distributed in powder-fine crystalline dolostone with residual texture (Figure 2(c)) and relatively good connectivity (Figure 2(d)). Early studies show that the intercrystalline pores of dolomite are mainly formed because of a "volume reduction effect." In particular, when the metasomatism of permeable granular

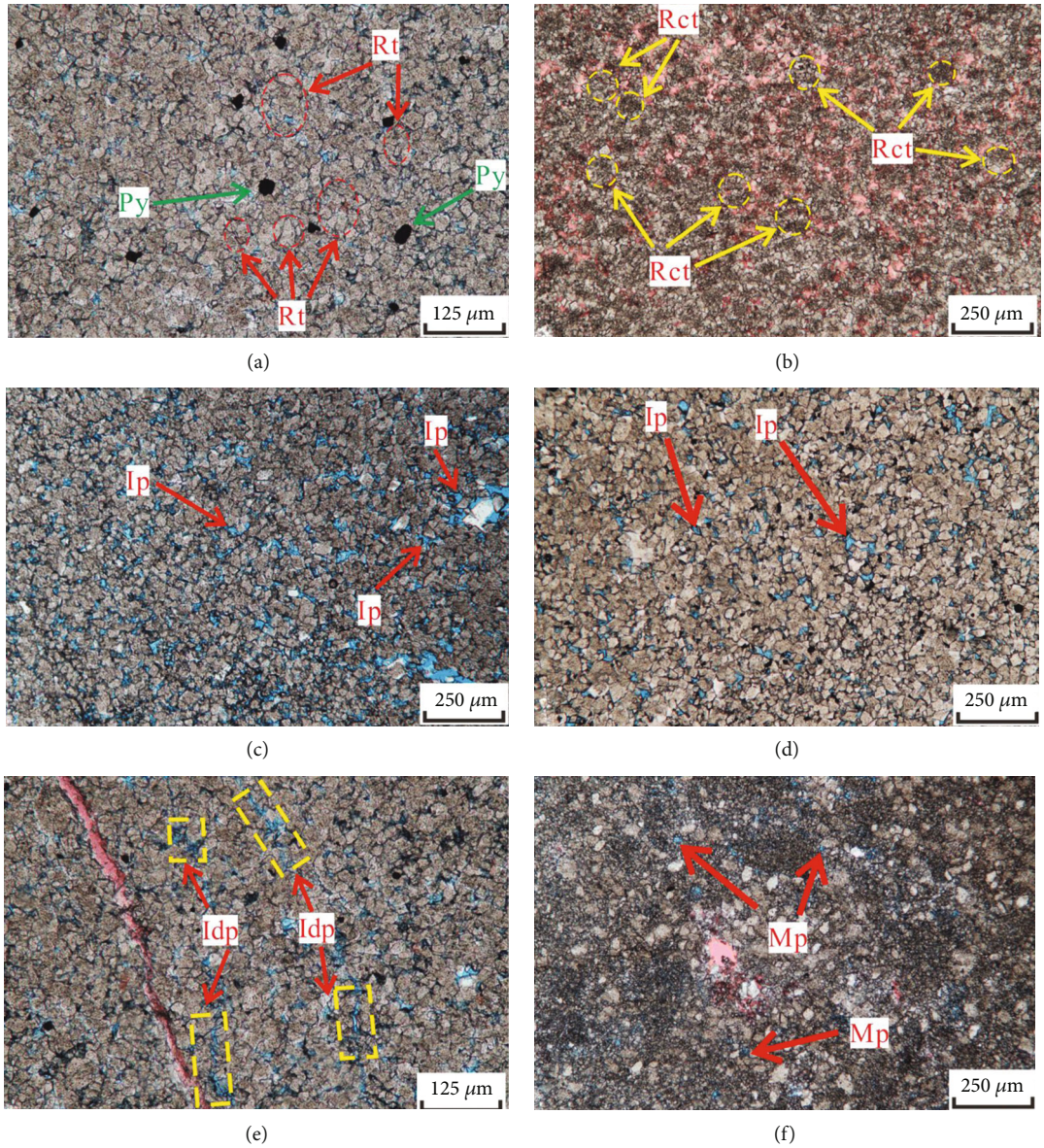

Figure 2: Microphotographs showing the petrographic characteristics of the intercrystalline pore-type dolostone reservoir in the submember $Ma5_5$ in the western Ordos Basin (IP = intercrystalline pore; Idp = intercrystalline dissolved pore; Mp = micropore; Rt = residual texture; Py = pyrite; Rct = residual chondrum structure). ((a) Powder-fine dolostone with oolitic texture, 4040.05 m, well Y1117; (b) powder-fine calcite-containing dolostone with chondrum structure, 4088.50 m, well Y1165; (c) intercrystalline pore, 3710.80 m, well S22; (d) intercrystalline pore, 4040.50 m, well Y1117; (e) micropore, 3954.80 m, well Y1112; (f) intercrystalline dissolved pore, 4040.10 m, well Y1117).

limestone by dolomitization fluid in a shallow burial stage takes place, some space will be released by the process of Mg^{2+} instead of Ca^{2+} [37]. However, in recent years, researchers think that intercrystalline pore might be formed in the reflux seepage dolomitization of permeable granular limestone and the redissolution of some residual calcite components between dolomite crystals by acidic fluids in the formation [38–40]. With the enhancement of dissolution, different intercrystalline pores will be connected and formed intercrystalline dissolved pore (Figure 2(e)).

Micropores are commonly found in powder crystal dolostone with residual gravel texture, and their number is slightly less than that of intercrystalline pores. Micropores are mainly developed between dolomite crystals with scattered distribution (Figure 2(f)) and relatively poor connectivity. This maybe mainly due to the filling by other clastic materials in the original dolomite intergranular pores in the later diagenetic stage.

(3) Pore Structure. The porosity and permeability are well correlated with some pore structure parameters such as the maximum mercury saturation, displacement pressure, and maximum throat radius of the carbonate reservoir [35, 41–45]. This indicates that the pore structure characteristics of a carbonate reservoir can be effectively characterized by the above parameters. Therefore, in this paper, the above three parameters were used to analyze the pore structure features of the dolostone reservoir in the submember $Ma5_5$ in the

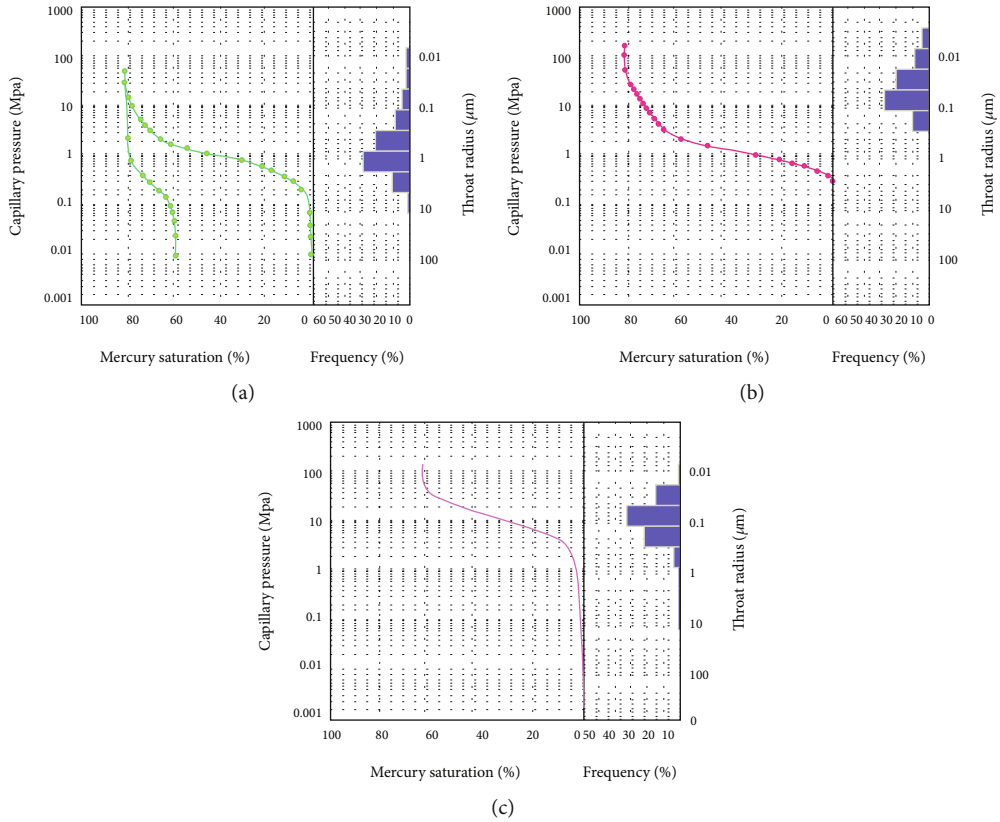

Figure 3: Pore structure of intercrystalline pore-type dolostone reservoir. ((a) MAMS pore structure, well S22, 3710.80 m; (b) MAFS pore structure, well Y1117, 4040.50 m; (c). MEFS pore structure, well Y1112, 3954.80 m).

study area. The pore structure of the intergranular pore dolostone reservoir can be categorized into three types: macropore-medium throat-single peak (MAMS), macropore-fine throat-single peak (MAFS), and medium pore-fine throat-single peak (MEFS).

MAMS pore structure is mainly developed in powder-fine dolostone with residual sand-cutting texture. The porosity and permeability corresponding to the MAMS pore structure in the study area are generally greater than 5% and $0.5 \times 10^{-3}\ \mu m^2$, respectively. Because of the increasing number and uniform distribution of dolomite intercrystalline pores, the storage capacity increases gradually, and the maximum mercury saturation is more than 70%. But, due to the fact that the throat of some intergranular pores is relatively narrow, the displacement pressure always ranges from 0.1 to 1 MPa (Figure 3(a)).

MAFS pore structure is also mainly developed in the powder-fine dolostone with residual sand-cutting texture. In this kind of pore structure, the number of dolomite intergranular pores with a narrow throat is generally greater than those of MAMS pore structure, which leads to the displacement pressure increasing with a value of more than 1 MPa (Figure 3(b)).

MEFS pore structure is commonly developed in powder-fine dolostone with residual sand-cutting texture and powder-crystal dolostone with residual gravel texture. Due to the increasing number of micropores in the rock, the maximum mercury saturation reduces and ranges from 50% to 70%, which is relatively lower than that of MAMS and MAFS pore structures. While the displacement pressure is still greater than that of 1 MPa might be resulted from the increasing number of intercrystalline pores with a fine throat (Figure 3(c)).

(4) Physical Property Characteristics. Based on the porosity and permeability analysis of nearly 40 intercrystalline pore-type dolostone samples in the study area, the porosity ranges from 2% to 11%, and the permeability is generally less than $0.5 \times 10^{-3}\ \mu m^2$. The cross-plots of porosity versus permeability display a relatively good correlation between them only when the porosity is greater than 5% (Figure 4), indicating that the connectivity of intercrystalline pores in this range is relatively better than in other ranges.

4.1.2. Dissolution Pore-Type Dolostone Reservoir

(1) Petrological Characteristics of Reservoir. The main rock type of the dissolution pore-type dolostone reservoir is powdery crystalline dolostone with gypsum and halite dissolution, which is mainly composed of powdery crystalline dolomite. These dolomites are primarily characterized by their content (between 79% and 99%), size (ranging from 0.005 to 0.05 mm), and automorphism degree (euhedral crystal or semi-euhedral crystal). The dissolved collapse breccia structure is commonly developed in this kind of dolostone

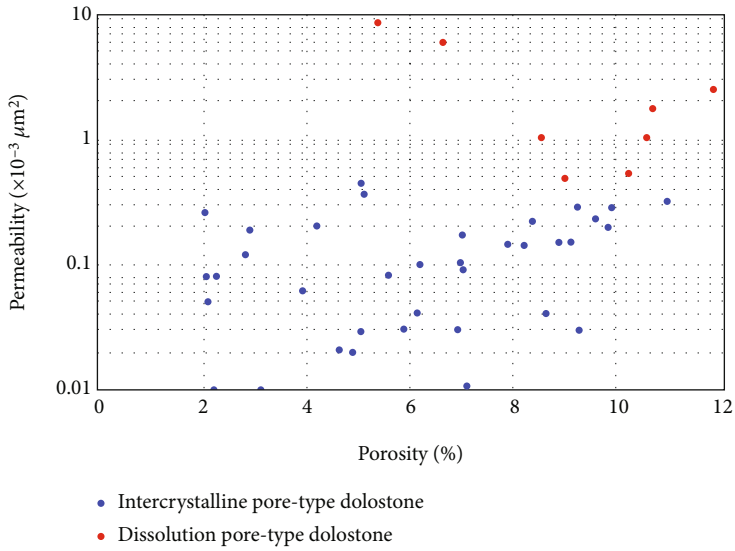

Figure 4: Cross-plot of porosity versus permeability of submember $Ma5_5$ in the study area.

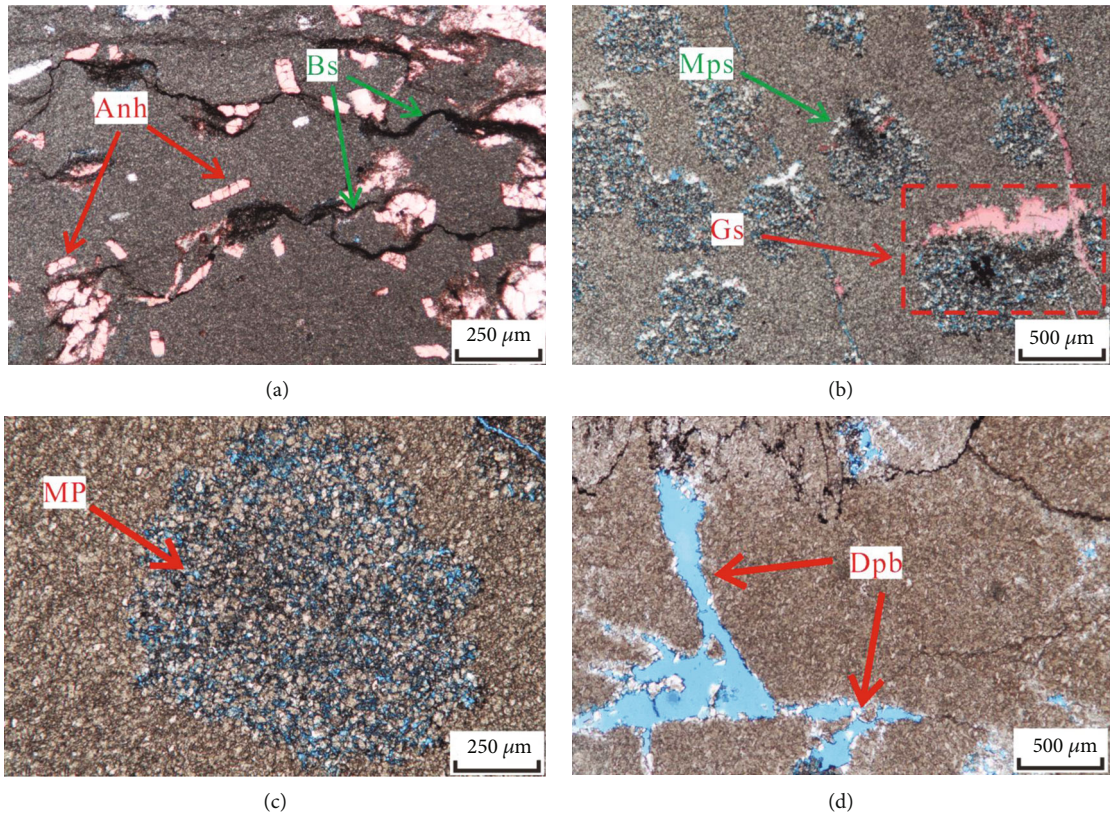

Figure 5: Lithofacies characteristics of dissolution pore-type dolostone reservoir. (Anh = anhydrite; Bs = breccia structure; Mps = moldic pore by salt dissolution; Gs = geopetal structure; Dpb = dissolved pore between breccias). ((a) Dissolved collapse breccia structure, 3859.85 m, well Y1112; (b) moldic pore by salt dissolution, and geopetal structure, 4089.80 m, well Y1165; (c) moldic pore, 4089.80 m, well Y1165; (d) dissolved pore between breccias, 3952.10 m, well Y1113).

(Figure 5(a)) and has the same component as the matrix, which is primarily powdery dolomite. In addition, this type of dolostone also shows typical petrographic features, including geopetal structure (Figure 5(b)) and some evaporate minerals such as lath-shaped anhydrite (Figure 5(a)).

(2) Pore Types and Genesis. The pore type of dissolution pore-type dolostone reservoir, primarily developed powdery crystalline dolostone with gypsum and halite dissolution, can be partitioned into moldic pore, dissolution pore between breccia, and dissolved microfractures.

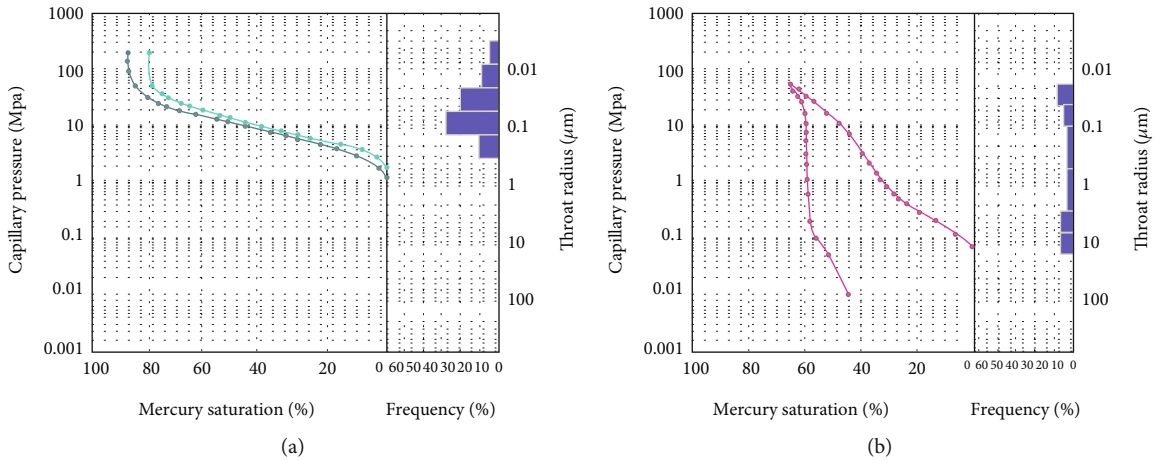

Figure 6: Pore structure of dissolution pore-type dolostone reservoir. ((a) MAFS pore structure, well Y1165, 4089.80 m; (b) MECM pore structure, well Y1113, 3952.10 m).

Moldic pore can be further divided into two types, including gypsum moldic pore and halite moldic pore. The formation mechanism describes below shows the anhydrite or halite associated with powdery crystal dolomite was easily dissolved after the dissolution of early freshwater, then formed dissolution pores (Figure 5(c)). Depending on the filling degree, such pores will change into different forms. To be specific, if these pores were not filled, they would be preserved to form some space with storage capacity. But, when parts of them were filled by surrounding rock debris, they would form a geopetal structure, of which in the upper part there is still a storage capacity.

The space between breccias will be filled by a large number of plaster components when a large amount of soluble matter in powdery crystalline dolostone with gypsum and halite dissolution were dissolved, causing dolostone strata to collapse and brecciate. But, these plaster components between breccias will be dissolved again by acid formation water to form dissolution pores between breccias when entered into the burial later stage (Figure 5(d)). In addition, some veins, which have been filled by plaster components in the early time, will also be dissolved by this acidic formation water to form dissolved microfractures. Even though these dissolved microfractures cannot provide enough space for storing petroleum or natural gas, they are of great significance for connecting different dissolution pores between breccias and improving reservoir permeability.

(3) Pore Structure. In the dissolution pore-type dolostone reservoir, part of the rock throats changes to be coarser, and the heterogeneity becomes stronger. As a result, macropore-fine throat-single peak (MAFS) and medium pore-coarse throat-multipeak (MECM) are two kinds of pore structures mainly developed in the dissolution pore-type dolostone reservoir.

The characteristics of the mercury injection parameters of the MAFS pore structure have been described above. It is worth noting that the MAFS pore structure developed in powdery crystalline dolostone with gypsum and halite dissolution resulted maybe from the better storage capacity of gypsum and halite moldic pores, which can keep a high maximum mercury saturation. However, the decreasing amount of matrix micropores and maximum throat radius lead to an increase in displacement pressure (Figure 6(a)).

The maximum mercury saturation of the MECM pore structure is in the range of 50% to 70%, and the displacement pressure is less than 0.01 MPa (Figure 6(b)). The powdery crystalline dolostone with gypsum and halite dissolution on which the MECM pore structure primarily formed mainly develops two kinds of pores, including moldic pores and dissolution pores between breccias. So, the mercury injection curve shows a multipeak feature. Due to a relatively decreasing number of moldic pores, the maximum mercury saturation of the reservoir increases. But, an increasing number of matrix micropores will lead to the maximum throat radius getting greater, which can cause a displacement pressure reduction.

(4) Physical Property Characteristics. The dissolution pore-type dolostone reservoir of the submember $Ma5_5$ has a relatively higher porosity (ranging from 5% to 12%) and permeability (greater than $0.5 \times 10^{-3}\ \mu m^2$) than those of the intercrystalline pore-type dolostone reservoir. But, an increasing number of dissolved microfractures in this kind of dolostone reservoir, which majorly improves the permeability (Figure 4), leads to a poor correlation between porosity and permeability.

5. Discussion

5.1. Reservoir Formation Mechanism

5.1.1. Intercrystalline Pore-Type Dolostone Reservoir. Based on the petrographic characteristics and the pore genesis analysis, the formation mechanism of an intercrystalline pore-type dolostone reservoir might be explained as follows. At first, the initial grain of limestone was deposited but without being strongly compacted, and a large number of

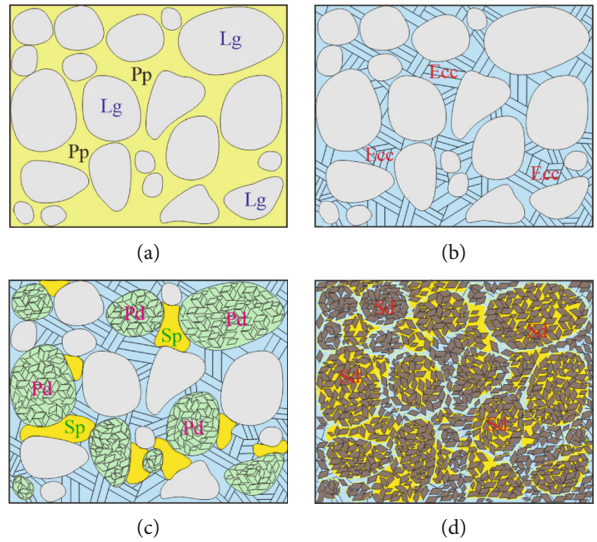

Figure 7: Schematic diagram of the formation mechanism of intercrystalline pore-type dolostone reservoir (after [18]) (Pp = primary intergranular pore; Lg = limestone grain; Ecc = early calcite cement; Pd = powdery intercrystalline dolomite; Sp = secondary pore; Sd = fine-crystal dolomite).

original intergranular pores between limestone particles were still preserved at the same time (Figure 7(a)). Then, with an increase in temperature and pressure, the early cementation started and resulted in the formation of calcite cement between the particles [18] (Figure 7(b)). After this, the magnesium-rich dolomitizing fluid formed by evaporation in the overlying strata refluxed into the permeable grain limestone, resulting in the dolomitization of the limestone particles and the formation of dolomite (Figure 7(c)). Meanwhile, some calcite components were still left in the intergranular pores between dolomite particles, and these calcite components will be dissolved by acidic formation fluids in the later stage to form dolomite intercrystalline pores [18, 46, 47]. With the continuous strengthening of the dissolution, the number of dolomite intercrystalline pores gradually increased (Figure 7(d)) and finally formed an intercrystalline pore dolostone reservoir.

5.1.2. Dissolution Pore-Type Dolostone Reservoir. Typical gypsum and halite moldic pores are primarily developed in the powdery crystalline dolostone with gypsum and halite dissolution, reflecting this dolostone deposited in an evaporation environment which has been suffered by freshwater. The dissolved breccia structure can also be seen in this kind of dolostone without a large amount of clay minerals filling the pores between breccia, indicating that the source of freshwater might be early freshwater rather than epigenetic freshwater. After an early freshwater dissolution, the powdery crystalline dolostone with gypsum and halite dissolution is not only subject to collapse and form breccia but also the components between breccias will be dissolved to form dissolution pores between breccias.

Therefore, the formation mechanism of the dissolution pore-type dolostone reservoir of the submember $Ma5_5$ in the study area can be described as follows. In the sedimentary or synsedimentary period, the sea level decreased relatively for a short time, resulting in an evaporation environment in the whole study area, and the powdery crystal dolostone containing gypsum and halite was deposited (Figure 8(a)). Due to a long time of exposure to the surface, gypsum and halite in dolostone were selectively dissolved by atmospheric freshwater or mixed water to form gypsum and halite moldic pores with a scattered distribution (Figure 8(b)), which are the major storage space of the dissolution pore-type dolostone reservoir (Figure 8(c)). In addition, the dissolution of these evaporated minerals in the dolostone interlayer leads to the collapsing and brecciation of the dolostone bed. Then the soluble components between breccias were dissolved again by formation water to form dissolution pores between breccias (Figure 8(d)), which improved the reservoir capacity.

5.2. Main Controlling Factors of Reservoir. Many previous studies have been carried out on the controlling factors of many kinds of natural gas enrichment [48, 49], but in fact, the distribution law of natural gas cannot be separated from the study of reservoir distribution. Therefore, the analysis of the controlling factors of the reservoir distribution is of significance.

5.2.1. Main Controlling Factors on Intercrystalline Pore-Type Dolostone Reservoir

(1) Lithofacies Palaeogeographic Environment. The original sedimentary environment (lithofacies palaeogeographic environment) not only provides the original carbonate rock property but also a basic environmental condition for the evolution of transforming from limestone to a dolostone reservoir. For example, the original intergranular pores developed in grain limestone deposited in the shoal microfacies environment of the platform margin or beach bar of an open platform provide an important migration channel for dolomitization fluid [50]. The lithofacies palaeogeographic environment is also of great significance to the formation of carbonate reservoir. According to the "single factor analysis

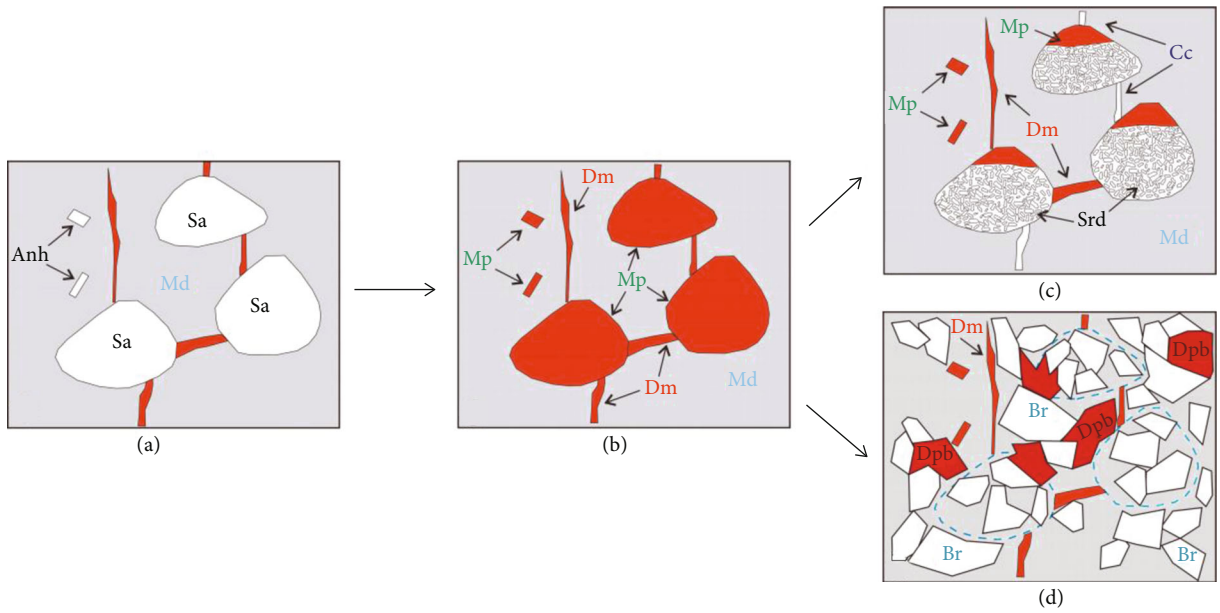

Figure 8: Schematic diagram of formation mechanism of dissolution pore-type dolostone reservoir (Anh = anhydrite; Sa = halite; Md = dolomicrite; Mp = moldic pore; Dm = dissolution microfracture; Srd = surrounding debris; Cc = calcite cement; Br = breccia structure; Dpb = dissolved pore between breccias). ((a) Powdery crystal dolostone containing gypsum and halite; (b) gypsum and halite moldic pores; (c) geopetal structure; (d) dissolution pores between breccias).

and multifactor comprehensive mapping method" [51], the lithofacies palaeogeographic environment of submember $Ma5_5$ in the study area was reconstructed in combination with the petrological indicators. The major principle we adopted to restore the lithofacies palaeogeography can be described briefly below. The fine crystalline dolostone displays a residual structure of the original granular limestone, and some calcitic components are still remained between dolomite crystals, reflecting a result of the gradual metasomatism process of dolomitizing fluids for the permeable granular limestone along a platform edge to the basin. Therefore, the paleogeographic environment should be a shoal at the platform edge. Leopard dolostone shows a typical biological disturbance structure, demonstrating a dolomitization process along the biological drilling holes. It reflects the shallow sea microfacies of an open sea platform, in which biodisturbed limestone mainly developed [52, 53]. So, the lithofacies palaeogeography should be an open sea platform. The result shows that two kinds of palaeogeographic environments are primarily developed in the study area, including platform edge and open sea platform, respectively, distributed in the west and south parts and in the central and eastern parts (Figure 9(a)). In specific, the platform edge is dominated by shoal microfacies with an original rock of grain limestone, while the open platform subfacies are dominated by the subtidal zone and beach bar with original rocks of biological limestone and grain limestone, respectively.

The multimineral logging model and the superposition map of reservoir thickness and lithofacies palaeogeographic distribution were used for the interpretation of the reservoir, the relationship between carbonate reservoir, and lithofacies palaeogeographic environment, respectively. The reservoir can be distinguished from the nonreservoir by using gamma, sonic, density, and neutron logging curves, as well as a porosity cutoff of 2%. The specific steps can be described as below. Firstly, the gamma curve should coincide with the sonic, density, and neutron logging curves in the mudstone site in a single well. Then, the curve separation degree can be used to quickly reflect the reservoir's physical property quality, and the greater the curve separation degree, the better the reservoir physical property. The results show that the carbonate reservoirs are almost distributed in the shoal microfacies, reflecting the distribution area of the carbonate reservoir in the submember $Ma5_5$ of the study area is basically controlled by the lithofacies paleogeographic environment, especially the shoal distribution area. It can be interpreted as follows. Firstly, the grain limestone with a good permeability is deposited in the shoal, and then the concentrated brine (dolomitizing fluid) coming from the upper strata formed in an evaporated environment will seep down from the edge to the interior of the platform when the sea level drops briefly. This resulted in the metasomatism of the calcite components in grain limestone by dolomitizing fluid, which formed a large number of dolostone and provided the basic formation condition for an intercrystalline pore-type dolostone reservoir. In addition, well A, well B, well C, and well S54 in the study area show a gas yield of 956000, 461000, 21000, and 271 m^3/d, respectively. This proves that more well is close to the shoal, more it is higher in gas yield.

(2) Active Reflux Seepage Dolomitization. Submember $Ma5_5$ in the study area has undergone multistage diagenesis, including early atmospheric freshwater dissolution, active reflux seepage dolomitization in the shallow burial period, latent reflux seepage dolomitization, and epigenetic karstification

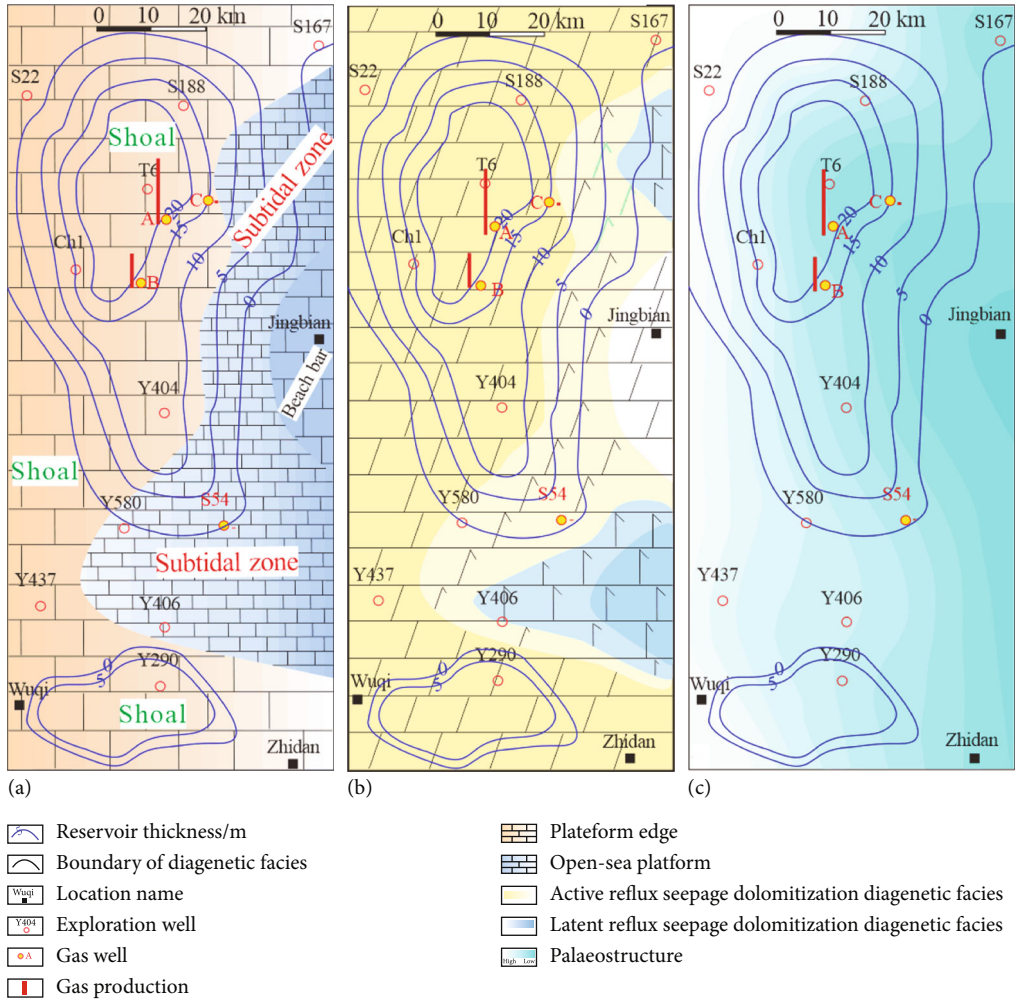

Figure 9: Relationship between different controlling factors and distribution of reservoir. ((a) Relationship between lithofacies palaeography and distribution of reservoir; (b) relationship between diagenetic facies and distribution of reservoir; (c) relationship between palaeostructure (top of the submember $Ma5_5$) and distribution of reservoir).

[25]. Among them, the active reflux seepage dolomitization makes the greatest contribution to the formation of intercrystalline pore-type dolostone reservoir due to its process of Mg^{2+} metasomatism with Ca^{2+}. During this process, a large number of dolomite crystals will be formed after the active reflux seepage dolomitization of grain limestone, and certain pores will be produced between dolomite crystals, which were generally filled at first by calcite components. But, a large number of dolomite intercrystalline pores will be formed when these calcite components are dissolved again by later formation acid fluids. The active reflux seepage dolomitization, mainly characterized by forming the powder-fine dolostone with residual structure, is the key to the formation of dolomite intercrystalline pores, which is also verified on the superposition map of diagenetic facies and reservoir thickness. For example, the dominant diagenetic facies in the study area is the active reflux seepage dolomitization subfacies, followed by the latent reflux seepage dolomitization (primarily featured by forming the leopard dolostone or leopard limestone) subfacies distributed in the northeast and southeast, while almost all the thick dolostone reservoirs (with a thickness greater than 10 m) are distributed in the active reflux seepage dolomitization subfacies zone (Figure 9(b)), in which the high gas yield wells are primarily located.

5.2.2. Main Controlling Factors on Dissolution Pore-Type Dolostone Reservoir

(1) Relatively High Part of Paleo-Uplift. Paleo-uplift is one of the important structural units controlling oil and natural gas accumulation in sedimentary basins [54]. At the end of the Ordovician Majiagou formation, the whole Ordos Basin displays a gradually decreasing structural trend from the central paleo-uplift to the eastern Mizhi Depression [32]. This structural condition controlled the sedimentary pattern of the Majiagou formation for a long time [33], resulting in an indirect relationship between structure and the distribution of different lithofacies.

The palaeostructure characteristics of the submember $Ma5_5$ in the study area were restored by using the residual stratigraphic thickness data coming from the top of the

submember $Ma5_5$ to the bottom of the Taiyuan formation. The overlying residual stratigraphic thickness ranges from 60 to 180 m, and the greater stratigraphic thickness is the low position of palaeostructure. The results show that the northern area represented by the S22-T6-S188-Ch1 well block in the study area displays a relative uplift along the NW-SE direction. While the central area represented by the Y404-Y580-S54 well block shows a relatively gentle uplift, the southern area represented by the Y437-Y406-Y290 well block is characterized by a slightly concave-uplift trend.

The superposition map of reservoir thickness and paleostructure shows that the largest and widest reservoirs are primarily distributed in the northern paleostructural uplift area rather than in the southern regions (Figure 9(c)). This suggests that the paleostructural uplift is the most favorable condition for carbonate reservoir development, which can be explained as follows. The high part of the paleostructure is more helpful to form an evaporation environment with a large number of evaporate minerals deposited, providing a material condition for the occurrence of selective dissolution of freshwater in the later stage. This can also be verified by the natural gas yield data of well A and well B which are located in the high part of the paleo-uplift.

(2) Freshwater Dissolution. Due to the fact that the strata are exposed to the highest part of the structure, they underwent freshwater dissolution more easily. So, it is easier for the gypsum and halite developed in the dolostone to be dissolved selectively by freshwater to form moldic pores after the formation of the powdery dolostone containing gypsum and halite. These moldic pores provided the major storage space of the dissolution pore-type dolostone reservoir. The subsequent rock collapse and brecciation provided the basic conditions for the formation of dissolved pores between breccias.

6. Conclusion

(1) There are two kinds of reservoirs of the submember $Ma5_5$ developed in the western Ordos Basin, including intercrystalline pore-type dolostone reservoir and dissolution pore-type dolostone reservoir. The former reservoir type is primarily powder-fine dolostone with residual structure, characterized by the pore types of dolomite intercrystalline pore and micropore with a porosity ranging from 2% to 11%, and three types of pore structure such as MAMS, MAFS, and MEFS. The latter reservoir type is mainly powdery crystalline dolostone with gypsum and halite dissolution, featured by the pore types of moldic pore and dissolved pore between breccias with a porosity greater than 5% and two types of pore structures such as MAFS and MECM

(2) The intercrystalline pore-type dolostone reservoir is mainly controlled by the lithofacies palaeogeographic environment and diagenesis. In specific, the shoal microfacies at the edge of the platform are the basic sedimentary environment condition for reservoir formation, and the active reflux seepage dolomitization is the key to reservoir formation. The dissolution pore-type dolostone reservoir is primarily influenced by both paleostructure and diagenesis. Concretely, the relatively high part of the paleo-uplift provides favorable conditions for the formation of evaporate minerals, and the early freshwater dissolution is the key to reservoir formation

Data Availability

All data that support the conclusions of this study are available from the corresponding author upon reasonable request.

Conflicts of Interest

The authors declare that the paper does not have any conflict of interest with other units and individuals.

Acknowledgments

This study was supported by the Fundamental Research Funds for the Central Universities (no. JZ2021HGQB0284), the National Natural Science Foundation of China (no. 91962218), the National 13th Five-Year Plan for Science and Technology Major Project of China (no. 2017ZX05005-002-004), and the Science and Technology Project of Hebei Education Department (no. ZD2022057).

References

[1] Z. Yuan, H. L. Yuan, Y. F. Fan, Q. C. Wang, and Y. Q. Guo, "Carbonate reservoir evaluation and gas bearing prediction in Ordos Basin," *Arabian Journal of Geosciences*, vol. 13, no. 17, p. 824, 2020.

[2] H. Liu, X. C. Tan, L. Li, B. Luo, C. L. Ma, and L. G. Yang, "Characteristics and main controlling factors of porous carbonate reservoirs: a case from the Jia 5 member of the Jialingjiang formation, southwest Sichuan Basin," *Petroleum Exploration and Development*, vol. 38, no. 3, pp. 275–281, 2011.

[3] W. Yang, W. R. Xie, G. Q. Wei et al., "Sequence lithofacies paleogeography, favorable reservoir distribution and exploration zones of the Cambrian and Ordovician in Sichuan Basin, China," *Acta Petrolei Sinica*, vol. 33, no. S2, pp. 21–34, 2012.

[4] M. Y. Hu, M. Deng, Z. G. Hu, and D. Xue, "Reservoir characteristics and main control factors of the carboniferous Huanglong formation in Sichuan Basin," *Earth Science Frontiers*, vol. 22, no. 3, pp. 310–321, 2015.

[5] B. Q. Li, Q. C. Wang, X. L. Zhang et al., "Characteristics of lithofacies paleogeography and its effect on the Majiagou submember $5_{1\text{-}2}$ reservoir in the central-southern Ordos Basin," *Acta Sedimentologica Sinica*, vol. 37, no. 3, pp. 589–600, 2019.

[6] X. L. Bai, Y. M. Yang, Y. Yang, L. Wen, and B. Luo, "Characteristics and controlling factors of high-quality dolomite reservoirs in the Permian Qixia formation, northwestern Sichuan," *Journal of Southwest Petroleum University (Science & Technology Edition)*, vol. 41, no. 1, pp. 47–56, 2019.

[7] N. N. Zhang, D. F. He, Y. P. Sun, and H. W. Li, "Distribution patterns and controlling factors of giant carbonate rock oil

and gas fields worldwide," *China Petroleum Exploration*, vol. 19, no. 6, pp. 54–65, 2014.

[8] A. J. Shen, W. Z. Zhao, A. P. Hu, M. She, Y. N. Chen, and X. F. Wang, "Major factors controlling the development of marine carbonate reservoirs," *Petroleum Exploration and Development*, vol. 42, no. 5, pp. 597–608, 2015.

[9] X. S. Wei, J. F. Ren, J. X. Zhao et al., "Paleo-geomorphologic characteristic evolution and geological significance of the Ordovician weathering crust in eastern Ordos Basin," *Acta Petrolei Sinica*, vol. 38, no. 9, pp. 999–1009, 2017.

[10] L. W. Zhu, Z. L. Wang, B. Zhang et al., "Characteristics of paleogeomorphology and paleokarstification and the impact on natural gas accumulation: a case study of upper assemblage of Majiagou formation in central Sulige gas field, Ordos Basin, China," *Carbonates and Evaporites*, vol. 34, no. 4, pp. 1353–1366, 2019.

[11] J. W. Cao, Z. W. Tang, Q. Y. Zhang, and Y. Dan, "Paleogeomorphic genesis assembly method for paleogeomorphic recovery in the major region of the Tahe oil field, Tarim Basin, northwest China," *Carbonates and Evaporites*, vol. 34, no. 2, pp. 283–295, 2019.

[12] B. Jiu, W. H. Huang, N. N. Mu, and Y. Li, "Types and controlling factors of Ordovician paleokarst carbonate reservoirs in the southeastern Ordos Basin, China," *Journal of Petroleum Science and Engineering*, vol. 198, no. 3, article 108162, 2020.

[13] H. X. Cao, H. Y. Wu, X. M. Ren, Y. Wu, Q. S. Liang, and M. Q. Hong, "Karst paleogeomorphology and reservoir distribution pattern of Ordovician in the southeastern Ordos Basin," *China Petroleum Exploration*, vol. 25, no. 3, pp. 146–155, 2020.

[14] R. C. Xie, Z. Wen, C. Zhang, T. Lei, S. Yin, and Z. W. Luo, "Characteristics, influencing factors, and prediction of fractures in weathered crust karst reservoirs: a case study of the Ordovician Majiagou formation in the Daniudi gas field, Ordos Basin, China," *Geological Journal*, vol. 55, no. 12, pp. 7790–7806, 2020.

[15] G. T. Wang, L. H. Cheng, D. W. Meng et al., "Characterization and formation of the Ordovician tight paleokarst carbonates in the eastern Ordos Basin and its gas accumulation," *Oil & Gas Geology*, vol. 39, no. 4, pp. 685–695, 2018.

[16] J. Xiao, H. C. Ji, J. X. Liu, Q. Guo, F. Yang, and C. Fang, "Diagenesis and its effect to carbonate reservoirs of the Ordovician in Dongpu area, Bohai Bay basin," *Journal of Palaeogeography*, vol. 20, no. 2, pp. 299–310, 2018.

[17] B. Q. Li, Q. C. Wang, X. L. Zhang et al., "Characteristics of diagenetic facies and its effect on the reservoir of $M5_5$~$M5_1$ submembers of Majiagou formation in central-southern Ordos Basin," *Journal of Northwest University(Natural Science Edition)*, vol. 48, no. 2, pp. 255–260, 2018.

[18] Q. Q. Luo, B. Liu, W. M. Jiang et al., "Diagenesis and pore evolution of dolomite reservoir in the 5th member of the Ordovician Majiagou formation, central Ordos Basin," *Oil & Gas Geology*, vol. 41, no. 1, pp. 102–115, 2020.

[19] F. A. Aljuboori, J. H. Lee, K. A. Elraies, and K. D. Stephen, "The impact of diagenesis precipitation on fracture permeability in naturally fractured carbonate reservoirs," *Carbonates and Evaporites*, vol. 36, no. 1, pp. 1–16, 2021.

[20] L. W. Qiu, T. Chang, Y. G. Zhang et al., "Main controlling factors and development model of high-quality carbonate reservoir in Yidong area," *Journal of Northeast Petroleum University*, vol. 40, no. 4, pp. 1–10, 2016.

[21] Z. Yu, Z. C. Ding, L. H. Wang et al., "Main factors controlling formation of dolomite reservoir underlying gypsum-salt layer in the 5th member of Ordovician Majiagou formation, Ordos Basin," *Oil & Gas Geology*, vol. 39, no. 6, pp. 1213–1224, 2018.

[22] H. X. Lan, M. Y. Fu, H. C. Deng et al., "Reservoir types and genesis of the Majiagou formation Daniudi gas field, Ordos Basin," *Acta Sedimentologica Sinica*, vol. 39, no. 6, pp. 1609–1621, 2021.

[23] Y. D. Zhang, W. Zhou, K. Deng, C. L. Wang, Y. Wang, and X. Y. Meng, "Palaeogeomorphology and reservoir distribution of the Ordovician karstified carbonate rocks in the structurally-gentle Gaoqiao area, Ordos Basin," *Acta Petrologica Sinica*, vol. 30, no. 3, pp. 757–767, 2014.

[24] Z. T. Su, H. D. Chen, F. Y. Xu, and X. Q. Jin, "Genesis and reservoir property of lower Ordovician Majiagou dolostones in Ordos Basin," *Marine Origin Petroleum Geology*, vol. 18, no. 2, pp. 15–22, 2013.

[25] Q. C. Wang, S. P. Zhao, Q. L. Wei et al., "Marine carbonate reservoir characteristics of the middle Ordovician Majiagou formation in Ordos Basin," *Journal of Palaeogeography*, vol. 14, no. 2, pp. 229–242, 2012.

[26] M. Liu, X. Q. Ding, Y. L. Wan, X. L. Bai, Q. Q. Chen, and J. P. Le, "Characteristics and distribution of Ordovician weathering crust reservoirs in Daniudi gas field, Ordos Basin," *Marine Origin Petroleum Geology*, vol. 19, no. 1, pp. 35–42, 2014.

[27] H. C. Jia and X. Q. Ding, "Characteristics of dolomite karst reservoirs in the $M5_{1+2}$ member of Majiagou formation, Daniudi gasfield, Ordos Basin, China," *Journal of Chengdu University of Technology (Science & Technology Edition)*, vol. 43, no. 4, pp. 415–422, 2016.

[28] T. Lei, H. C. Deng, D. Wu et al., "Depositional model of the lower-middle Ordovician Majiagou formation in Daniudi gas field, Ordos Basin," *Journal of Palaeogeography*, vol. 22, no. 3, pp. 523–538, 2020.

[29] X. H. Ma, "Natural gas exploration and development situation in Ordos Basin, NW China," *Petroleum Exploration & Development*, vol. 32, no. 4, pp. 50–53, 2005.

[30] Y. P. Wu and Y. C. Wang, "Factors influencing natural gas enrichment in Jingbian gas field, Ordos Basin," *Oil & Gas Geology*, vol. 28, no. 4, pp. 473–478, 2007.

[31] H. Bai, T. B. Yang, K. F. Hou, Z. X. Ma, and M. Feng, "Main controlling factors and gas enrichment area selection of $Ma5_5$ gas reservoir in eastern Sulige gas field," *Xinjiang Petroleum Geology*, vol. 43, no. 3, pp. 271–277, 2022.

[32] F. H. Hou, S. X. Fang, J. S. Zhao et al., "Depositional environment model of middle Ordovician Majiagou formation in Ordos Basin," *Marine Origin Petroleum Geology*, vol. 7, no. 1, pp. 38–46, 2002.

[33] Y. Xiong, L. Li, C. X. Wen et al., "Characteristics and genesis of Ordovician $Ma5_{1+2}$ sub-member reservoir in northeastern Ordos Basin," *Oil & Gas Geology*, vol. 37, no. 5, pp. 691–701, 2016.

[34] W. H. Li, Q. Chen, Z. C. Li, R. G. Wang, Y. Wang, and Y. Ma, "Lithofacies palaeogeography of the early Paleozoic in Ordos area," *Journal of Palaeography*, vol. 14, no. 1, pp. 85–100, 2012.

[35] B. Q. Li, "*Characteristics and identification of diagenetic facies of low permeability and ultra-low permeability dolostone reservoirs*," Northwest University, 2020.

[36] Z. Z. Feng, *China Sedimentology*, Petroleum Industry Press, Beijing, 1994.

[37] P. K. Weyl, "Porosity through dolomitization: conservation-of-mass requirements," *Journal of Sedimentary Petrology*, vol. 30, no. 1, pp. 85–90, 1960.

[38] T. Vahid and J. Adeleh, "Porosity evolution in dolomitized Permian-Triassic strata of the Persian Gulf, insights into the porosity origin of dolomite reservoirs," *Journal of Petroleum Science and Engineering*, vol. 181, article 206191, 2019.

[39] Z. T. Su, W. She, H. H. Liao, S. L. Hu, G. Q. Liu, and H. Ma, "Research progress and development trend of the genesis of dolomite reservoirs," *Natural Gas Geoscience*, vol. 33, no. 7, pp. 1175–1188, 2022.

[40] J. G. Zhou, Z. Yu, D. X. Wu et al., "Restoration of formation processes of dolomite reservoirs based on laser U-Pb dating: a case study of Ordovician Majiagou formation, Ordos Basin, NW China," *Petroleum Exploration and Development*, vol. 49, no. 2, pp. 285–295, 2022.

[41] W. M. Ji, F. Hao, H. M. Schulz, Y. Song, and J. Tian, "The architecture of organic matter and its pores in highly mature gas shales of the lower Silurian Longmaxi formation in the upper Yangtze platform, South China," *AAPG Bulletin*, vol. 102, no. 12, pp. 2909–2942, 2019.

[42] H. X. Huang, R. X. Li, F. Y. Xiong et al., "A method to probe the pore-throat structure of tight reservoirs based on low- field NMR: insights from a cylindrical pore model," *Marine and Petroleum Geology*, vol. 117, article 104344, 2020.

[43] H. X. Huang, R. X. Li, W. T. Chen et al., "Revisiting movable fluid space in tight fine-grained reservoirs: a case study from Shahejie shale in the Bohai Bay basin, NE China," *Journal of Petroleum Science & Engineering*, vol. 207, article 109170, 2021.

[44] H. X. Huang, R. X. Li, Z. Lyu et al., "Comparative study of methane adsorption of Middle-Upper Ordovician marine shales in the western Ordos Basin, NW China: insights into impacts of moisture on thermodynamics and kinetics of adsorption," *Chemical Engineering Journal*, vol. 446, article 137411, 2022.

[45] K. Zhang, Y. Song, Z. X. Jiang et al., "Quantitative comparison of genesis and pore structure characteristics of siliceous minerals in marine shale with different TOC contents-a case study on the shale of lower Silurian Longmaxi formation in Sichuan Basin, southern China," *Frontiers in Earth Science*, vol. 43, no. 3, article 887160, 2022.

[46] W. Z. Zhao, A. J. Shen, J. F. Zheng, Z. F. Qiao, X. F. Wang, and J. M. Lu, "The porosity origin of dolostone reservoirs in the Tarim, Sichuan and Ordos basins and its implication to reservoir prediction," *Science China: Earth Sciences*, vol. 44, no. 9, pp. 1925–1939, 2014.

[47] B. Q. Li, Z. Z. Wu, T. F. Zhou, B. Chen, Q. C. Wang, and X. L. Zhang, "Constraints on diagenetic fluid source and genesis in tight dolostone reservoir of submember Ma55 of Ordovician Majiagou formation in northwestern Ordos Basin, China: evidence from petrology and geochemistry," *Geofluids*, vol. 2022, Article ID 8430179, 13 pages, 2022.

[48] L. Chen, K. Y. Liu, S. Jiang, H. X. Huang, J. Q. Tan, and L. Zuo, "Effect of adsorbed phase density on the correction of methane excess adsorption to absolute adsorption in shale," *Chemical Engineering Journal*, vol. 420, article 127678, 2021.

[49] L. Chen, L. Zuo, Z. X. Jiang et al., "Mechanisms of shale gas adsorption: evidence from thermodynamics and kinetics study of methane adsorption on shale," *Chemical Engineering Journal*, vol. 361, pp. 559–570, 2019.

[50] B. Ning, Q. C. Wang, B. Q. Li, Y. F. Zhu, C. G. Jin, and Z. Yan, "Genetic model for $M5_5$ sub-member dolomitization of Majiagou formation in Ordos Basin," *Xinjiang Petroleum Geology*, vol. 36, no. 5, pp. 531–538, 2015.

[51] Z. Z. Feng, "Single factor analysis and multifactor comprehensive mapping method- reconstruction of quantitative lithofacies palaeogeography," *Journal of Palaeography*, vol. 6, no. 1, pp. 3–19, 2004.

[52] Q. C. Wang, W. Wei, J. Zhao et al., "Geochemical characteristics of dolostone diagenetic facies of the Ordovician in Ordos Basin," *Journal of Palaeogeography*, vol. 19, no. 5, pp. 849–864, 2017.

[53] B. Q. Li, Q. C. Wang, and X. L. Zhang, "Petrographic and geochemical evidence of the diagenetic environment and fluid source of dolomitization of dolomite: a case study from the Ma55 to Ma51 submembers of the Ordovician Majiagou formation, central Yishan slope, Ordos Basin, China," *Carbonates and Evaporites*, vol. 35, no. 2, p. 36, 2020.

[54] K. Deng, S. N. Zhang, L. F. Zhou, and Y. Liu, "Formation and tectonic evolution of the Paleozoic central paleouplift of Ordos Basin and its implications for oil-gas exploration," *Geotectonica et Metallogenia*, vol. 35, no. 2, pp. 190–197, 2011.